

# UC San Diego

## UC San Diego Previously Published Works

### Title

The role of clusterin in amyloid- $\beta$ -associated neurodegeneration.

### Permalink

<https://escholarship.org/uc/item/9dr272x4>

### Journal

JAMA neurology, 71(2)

### ISSN

2168-6149

### Authors

Desikan, Rahul S  
Thompson, Wesley K  
Holland, Dominic  
[et al.](#)

### Publication Date

2014-02-01

### DOI

10.1001/jamaneurol.2013.4560

Peer reviewed

## Original Investigation

# The Role of Clusterin in Amyloid- $\beta$ -Associated Neurodegeneration

Rahul S. Desikan, MD, PhD; Wesley K. Thompson, PhD; Dominic Holland, PhD; Christopher P. Hess, MD, PhD; James B. Brewer, MD, PhD; Henrik Zetterberg, MD, PhD; Kaj Blennow, MD, PhD; Ole A. Andreassen, MD, PhD; Linda K. McEvoy, PhD; Bradley T. Hyman, MD, PhD; Anders M. Dale, PhD; for the Alzheimer's Disease Neuroimaging Initiative Group

**IMPORTANCE** Converging evidence indicates that clusterin, a chaperone glycoprotein, influences Alzheimer disease neurodegeneration. However, the precise role of clusterin in Alzheimer disease pathogenesis is still not well understood.


**OBJECTIVE** To elucidate the relationship between clusterin, amyloid- $\beta$  ( $A\beta$ ), phosphorylated tau (p-tau), and the rate of brain atrophy over time among nondemented older individuals.

**DESIGN, SETTING, AND PARTICIPANTS** This longitudinal cohort included cognitively normal older participants and individuals with mild cognitive impairment assessed with baseline lumbar puncture and longitudinal structural magnetic resonance imaging. We examined 241 nondemented older individuals from research centers across the United States and Canada (91 participants with a Clinical Dementia Rating score of 0 and 150 individuals with a Clinical Dementia Rating score of 0.5).

**MAIN OUTCOMES AND MEASURES** Using linear mixed-effects models, we investigated interactions between cerebrospinal fluid (CSF) clusterin, CSF  $A\beta_{1-42}$ , and CSF p-tau at threonine 181 (p-tau<sub>181p</sub>) on the atrophy rate of the entorhinal cortex and hippocampus.

**RESULTS** Across all participants, we found a significant interaction between CSF clusterin and CSF  $A\beta_{1-42}$  on the entorhinal cortex atrophy rate but not on the hippocampal atrophy rate. Cerebrospinal fluid clusterin was associated with the entorhinal cortex atrophy rate among CSF  $A\beta_{1-42}$ -positive individuals but not among CSF  $A\beta_{1-42}$ -negative individuals. In secondary analyses, we found significant interactions between CSF  $A\beta_{1-42}$  and CSF clusterin, as well as CSF  $A\beta_{1-42}$  and CSF p-tau<sub>181p</sub>, on the entorhinal cortex atrophy rate. We found similar results in subgroup analyses within the mild cognitive impairment and cognitively normal cohorts.

**CONCLUSIONS AND RELEVANCE** In nondemented older individuals,  $A\beta$ -associated volume loss occurs in the presence of elevated clusterin. The effect of clusterin on  $A\beta$ -associated brain atrophy is not confounded or explained by p-tau. These findings implicate a potentially important role for clusterin in the earliest stages of the Alzheimer disease neurodegenerative process and suggest independent effects of clusterin and p-tau on  $A\beta$ -associated volume loss.

 Supplemental content at [jamaneurology.com](http://jamaneurology.com)

*JAMA Neurol.* 2014;71(2):180-187. doi:10.1001/jamaneurol.2013.4560  
Published online December 30, 2013.

**Author Affiliations:** Author affiliations are listed at the end of this article.

**Group Information:** A list of Alzheimer's Disease Neuroimaging Initiative investigators can be found at [http://loni.usc.edu/ADNI/Data/ADNI\\_Authorship\\_List.pdf](http://loni.usc.edu/ADNI/Data/ADNI_Authorship_List.pdf).

**Corresponding Author:** Rahul S. Desikan, MD, PhD, Department of Radiology, University of California, San Diego, 8950 Villa La Jolla Dr, Ste C101, La Jolla, CA 92037-0841 (rdesikan@ucsd.edu).

Converging genetic, cellular, molecular, and biomarker evidence indicates that clusterin, a chaperone glycoprotein also known as apolipoprotein J, influences Alzheimer disease (AD) pathogenesis. Clusterin levels are increased in AD-affected brain regions<sup>1-3</sup> and elevated in the cerebrospinal fluid (CSF) of patients with AD.<sup>4</sup> Several genomewide association studies have identified clusterin gene variants as AD susceptibility loci.<sup>5</sup> Elevated plasma clusterin levels are associated with disease prevalence and severity of AD<sup>6</sup> and with increased amyloid deposition and brain atrophy.<sup>7</sup> Still, experimental findings suggest that clusterin increases both amyloid- $\beta$  (A $\beta$ ) aggregation and clearance,<sup>5</sup> leading to the question of whether elevated clusterin levels are beneficial or harmful.

In humans, structural magnetic resonance imaging (MRI) and CSF biomarkers allow for the indirect assessment of cellular changes underlying AD in vivo. Structural MRI provides measures of brain atrophy, which include loss of dendrites, synapses,<sup>8</sup> and neurons.<sup>9</sup> Low CSF levels of A $\beta$  strongly correlate with intracranial amyloid plaques, and high concentrations of CSF phosphorylated-tau (p-tau) correlate with tau-associated neurofibrillary tangles.<sup>10</sup> Here, we investigated whether interactions between increased CSF clusterin and decreased CSF A $\beta_{1-42}$  and increased CSF clusterin and increased CSF p-tau<sub>181p</sub> are associated with increased brain atrophy over time in nondemented older individuals at risk for developing AD. Building on recent evidence that A $\beta$ -associated volume loss occurs in the presence of elevated p-tau,<sup>11-15</sup> we also examined the additive effect on volume loss of an interaction between increased CSF clusterin and decreased CSF A $\beta_{1-42}$  in the presence of an interaction between increased CSF p-tau at threonine 181 (p-tau<sub>181p</sub>) and decreased CSF A $\beta_{1-42}$ .

## Methods

The institutional review boards of all participating institutions approved the procedures of this study, and written informed consent was obtained from all participants or their surrogates.

A total of 313 nondemented older participants from the Alzheimer's Disease Neuroimaging Initiative underwent longitudinal MRI and CSF lumbar puncture. Of these, we restricted analyses to 91 cognitively normal older adults (healthy control [HC] participants) and 150 individuals with amnesic mild cognitive impairment (MCI) who had a quality-assured baseline scan and at least 1 follow-up MRI scan (6 months-3.5 years, 4% with 6-month follow-up, 8% with 12-month follow-up, 11% with 18-month follow-up, 42% with 24-month follow-up, and 35% with 36-month follow-up) (Table; for additional details, see eAppendix 1 and eAppendix 2 in Supplement).

We examined baseline CSF clusterin levels derived from a multiplex-based immunoassay panel based on Luminex immunoassay technology developed by Rules-Based Medicine (MyriadRBM).<sup>16</sup> In brief, the Alzheimer's Disease Neuroimaging Initiative Biomarker Core assessed CSF samples (159 analytes measured by the MyriadRBM) from a total of 327 indi-

**Table. Demographic, Clinical, and Imaging Data for All Participants in This Study**

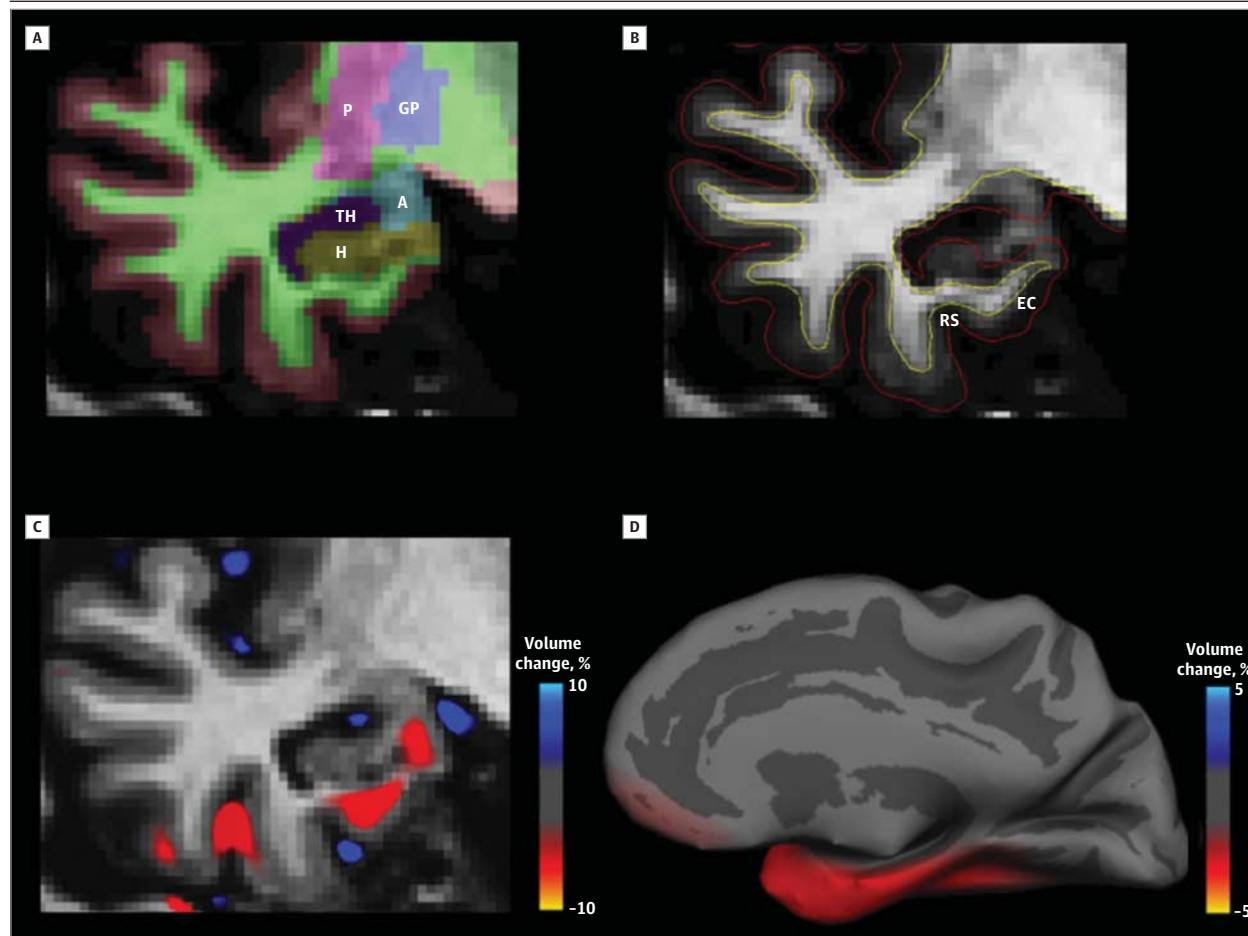
Characteristic	Mean (SE)	
	Cognitively Normal (n = 91)	Mild Cognitive Impairment (n = 150)
Age	76.0 (0.6)	75.1 (0.7)
Female, %	51	33
Education, y	15.6 (0.3)	16.1 (0.2)
MMSE score	29.1 (0.1)	26.7 (0.1)
CDR-SB score	0.03 (0.01)	1.5 (0.07)
APOE $\epsilon$ 4 carriers, %	24	54
CSF clusterin level, $\mu$ g/mL	1.39 (0.02)	1.42 (0.01)
CSF A $\beta_{1-42}$ level, pg/mL	207.8 (5.6)	157.5 (4.1)
CSF p-tau <sub>181p</sub> level, pg/mL	24.7 (1.4)	36.8 (1.3)
Baseline LP-MRI interval, mo	0.07 (0.007)	0.08 (0.006)
Time between baseline and last available MRI scans, y	2.37 (0.08)	2.17 (0.05)
Annualized percentage change		
Entorhinal cortex	-0.84 (0.11)	-2.37 (0.12)
Hippocampus	-0.95 (0.08)	-2.42 (0.13)
Amygdala	-0.99 (0.10)	-2.65 (0.15)
Middle temporal gyrus	-0.70 (0.09)	-1.97 (0.12)

Abbreviations: A $\beta_{1-42}$ , amyloid- $\beta$  1-42; APOE  $\epsilon$ 4, apolipoprotein E  $\epsilon$ 4 allele; CDR-SB, Clinical Dementia Rating-Sum of Boxes; CSF, cerebrospinal fluid; LP, lumbar puncture; MMSE, Mini-Mental State Examination; MRI, magnetic resonance imaging; p-tau<sub>181p</sub>, phosphorylated tau at threonine 181.

viduals. These baseline CSF samples had matching aliquots from 1 year, allowing evaluation of test-retest to determine analyte precision. For each analyte, a multistep quality-control procedure was implemented, which included evaluation of CSF signal characteristics (high, medium, and low), assessment for normality of distribution (abnormal values were transformed), and need for imputation (data with missing values and high/low values) (for additional details on CSF quality-control procedures, see the *Biomarkers Consortium Data Primer*<sup>16</sup>). We used the quality-controlled values for CSF clusterin in all analyses. Using previously proposed CSF cutoffs,<sup>17</sup> we examined baseline CSF A $\beta_{1-42}$  and p-tau<sub>181p</sub> levels and classified participants based on low (<192 pg/mL, positive) and high (>192 pg/mL, negative) A $\beta_{1-42}$  levels, and high (>23 pg/mL, positive) and low (<23 pg/mL, negative) p-tau<sub>181p</sub> levels. As previously described,<sup>17</sup> CSF A $\beta_{1-42}$  and p-tau<sub>181p</sub> were measured using the multiplex xMAP Luminex platform (Luminex Corp) with Innogenetics (INNOBIA AlzBio3) immunoassay kit-based reagents.

We analyzed 977 T1-weighted MRI scans using a modified version of the FreeSurfer software package (<http://surfer.nmr.mgh.harvard.edu>). These analysis procedures have been applied, validated, and described in detail in a number of publications.<sup>18</sup> The MRI scans were reviewed for quality, automatically corrected for spatial distortion due to gradient nonlinearity, registered, and averaged to improve the signal to noise ratio. The cortical surface was automatically reconstructed and gray matter thickness measurements were obtained at each point across the cortical mantle. Here, we primarily focused

Figure 1. T1-Weighted Magnetic Resonance Images



Images in the coronal dimension and a medial semi-inflated gray matter cortical surface depicting the hippocampus (A) and entorhinal cortex (B) and 1-year volume change fields (C and D) for a participant with mild cognitive impairment at the median for hippocampus and entorhinal cortex volume loss (annualized percentage change) who was amyloid- $\beta$  positive, phosphorylated tau positive, and demonstrated elevated clusterin levels. A, Automated segmentation of the baseline, structural magnetic resonance image with subcortical structures (including the hippocampus) depicted in various colors. B, The red overlay shows the gray matter/cerebrospinal fluid boundary, the white overlay depicts the gray/white matter boundary, and the distance between these surfaces

represents the cortical thickness. Here, we were primarily interested in evaluating longitudinal thinning of the entorhinal cortex. C, Heat map representation of the voxelwise estimates of volumetric change at 1 year. Note that volumetric change is most pronounced in the medial temporal lobe. D, Semi-inflated gray matter cortical surface (medial hemisphere) with a heat map representation of cortical volumetric change at 1 year. Note that volumetric change is most pronounced in the medial temporal and temporopolar cortices. A indicates amygdala; EC, entorhinal cortex; GP, globus pallidus; H, hippocampus; P, putamen; RS, rhinal sulcus; TH, temporal horn lateral ventricles.

on the entorhinal cortex and hippocampus, 2 medial temporal lobe regions that are affected in the earliest stages of AD (Figure 1).<sup>19</sup> We additionally evaluated the amygdala and middle temporal gyrus, 2 temporal lobe regions that are also affected in AD.<sup>19</sup> The entorhinal cortex and middle temporal gyrus were delineated using an automated, surface-based cortical parcellation atlas.<sup>20</sup> The hippocampus and amygdala were identified using an automated, subcortical segmentation atlas.<sup>21</sup> For the analysis of the longitudinal gray matter volume change, we used Quarc (quantitative anatomical regional change), a method developed from our laboratory.<sup>22,23</sup> Briefly, each participant's follow-up image was affine aligned to the baseline scan and locally intensity normalized. Using nonlinear registration, a deformation field was then calculated to locally register the images with high fidelity for both large- and small-scale structures including those with low

boundary contrast. From the deformation field, a volume-change field (atrophy) can directly be calculated. Using the baseline subcortical and cortical regions of interest, the volume-change field can be sampled at points across the cortical surface or averaged over subcortical regions to give the percentage volume change for those regions of interest (Figure 1).

We asked whether statistical interactions between CSF clusterin and CSF  $A\beta_{1-42}$  and between CSF clusterin and CSF p-tau<sub>181p</sub> are associated with brain atrophy over time (Figure 2). Using a linear mixed-effects model, we concurrently examined the main and interactive effects of CSF clusterin, CSF  $A\beta_{1-42}$ , and CSF p-tau<sub>181p</sub> on the atrophy rate of the temporal lobe regions (entorhinal cortex, hippocampus, amygdala, and middle temporal gyrus), covarying for age, sex, carrier status for the  $\epsilon 4$  allele of apolipoprotein E, group status (MCI vs HC), and disease severity (assessed using Clinical Dementia Rating-

Sum of Boxes, a composite measure that characterizes 6 domains of cognitive and functional performance<sup>24</sup>). Of note, the main effects of all variables (the 3 CSF analytes and all covariates) were also included in these analyses. For brevity, we focused on the effects of interest. Specifically:

$$\Delta v = \beta_0 + \beta_1 \Delta t + \beta_2 \text{CSF\_clusterin} \times \Delta t + \beta_3 \text{CSF\_A}\beta_{1-42\_status} \times \Delta t + \beta_4 \text{CSF\_p-tau}_{181p\_status} \times \Delta t + \beta_5 [\text{CSF\_clusterin} \times \text{CSF\_A}\beta_{1-42\_status} \times \Delta t] + \beta_6 [\text{CSF\_clusterin} \times \text{CSF\_p-tau}_{181p\_status} \times \Delta t] + \text{covariates} \times \Delta t + \epsilon.$$

In this equation 1,  $\Delta v$  indicates entorhinal cortex or hippocampal atrophy (millimeters)<sup>3</sup> and  $\Delta t$  indicates change in time from baseline MRI scan (years). Intercept and slope ( $\beta_0$  and  $\beta_1$ ) were entered as mixed effects.

Prior findings from our laboratory indicate that A $\beta$ -associated neurodegeneration occurs in the presence of elevated p-tau.<sup>11-13</sup> To test whether the effect of clusterin on A $\beta$ -associated neurodegeneration is independent from the effect of p-tau on A $\beta$ -associated neurodegeneration, we performed secondary analyses and fit the following linear mixed-effects model:

$$\Delta v = \beta_0 + \beta_1 \Delta t + \beta \text{CSF\_clusterin} \times \Delta t + \beta \text{CSF\_A}\beta_{1-42\_status} \times \Delta t + \beta \text{CSF\_p-tau}_{181p\_status} \times \Delta t + \beta [\text{CSF\_clusterin} \times \text{CSF\_A}\beta_{1-42\_status} \times \Delta t] + \beta [\text{CSF\_p-tau}_{181p\_status} \times \text{CSF\_A}\beta_{1-42\_status} \times \Delta t] + \text{covariates} \times \Delta t + \epsilon.$$

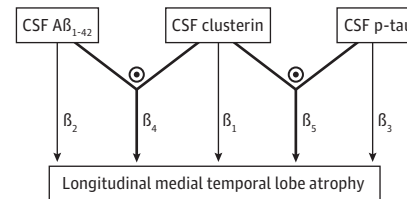
In this equation 2,  $\Delta v$  indicates entorhinal cortex or hippocampal atrophy (millimeters)<sup>3</sup> and  $\Delta t$  indicates change in time from baseline MRI scan (years). Intercept and slope ( $\beta_0$  and  $\beta_1$ ) were entered as mixed effects. We covaried for age, sex,  $\epsilon 4$  allele of apolipoprotein E carrier status, group status (MCI vs HC), and Clinical Dementia Rating-Sum of Boxes score. The main effects of all variables (the 3 CSF analytes and all covariates) were also included in these analyses.

To evaluate whether the just-described effects of interest between CSF clusterin, CSF A $\beta_{1-42}$  status, and CSF p-tau<sub>181p</sub> status were different between the MCI and HC cohorts, we performed additional analyses fitting group status (MCI vs HC) as an interaction with change in time from baseline MRI scan ( $\Delta t$  or time) and the main interactive effects. The main effects of all variables (the 3 CSF analytes and all covariates) were also included in these analyses.

## Results

Results from the primary analyses revealed a significant 3-way interaction between CSF clusterin, CSF A $\beta_{1-42}$  status, and time ( $\beta_5 = -0.032$ ; SE = 0.01;  $P = .01$ ), indicating that increased CSF clusterin and positive CSF A $\beta_{1-42}$  status were associated with an elevated entorhinal cortex atrophy rate. In contrast, the interaction between CSF clusterin, CSF p-tau<sub>181p</sub> status, and time was not significant ( $\beta_6 = 0.01$ ; SE = 0.01;  $P = .54$ ). With both of these 3-way interaction terms in the model, only the effect of CSF A $\beta_{1-42}$  status by time was significantly associated with the entorhinal atrophy cortex rate ( $\beta_3 = 0.04$ ; SE = 0.02;  $P = .02$ ); the effect of time by CSF clusterin and CSF p-tau<sub>181p</sub> status was not associated with the entorhinal cortex atrophy rate. None of the main effects of CSF clusterin, CSF A $\beta_{1-42}$  status, and CSF p-tau<sub>181p</sub> status were significant.

**Figure 2. Diagram of the Primary Hypotheses Evaluated in the Current Study Where the Primary Outcome Was Longitudinal Medial Temporal Lobe Atrophy**



The diagram shows the main effect of clusterin ( $\beta_1$ ), the main effect of amyloid- $\beta$  1-42 (A $\beta_{1-42}$ ) ( $\beta_2$ ), the main effect of phosphorylated tau (p-tau) ( $\beta_3$ ), an interactive effect between clusterin and A $\beta_{1-42}$  ( $\beta_4$  and circle with dot in the center), and an interactive effect between clusterin and p-tau ( $\beta_5$  and circle with dot in the center). CSF indicates cerebrospinal fluid. The circle with the dot in the center illustrates an interactive effect.

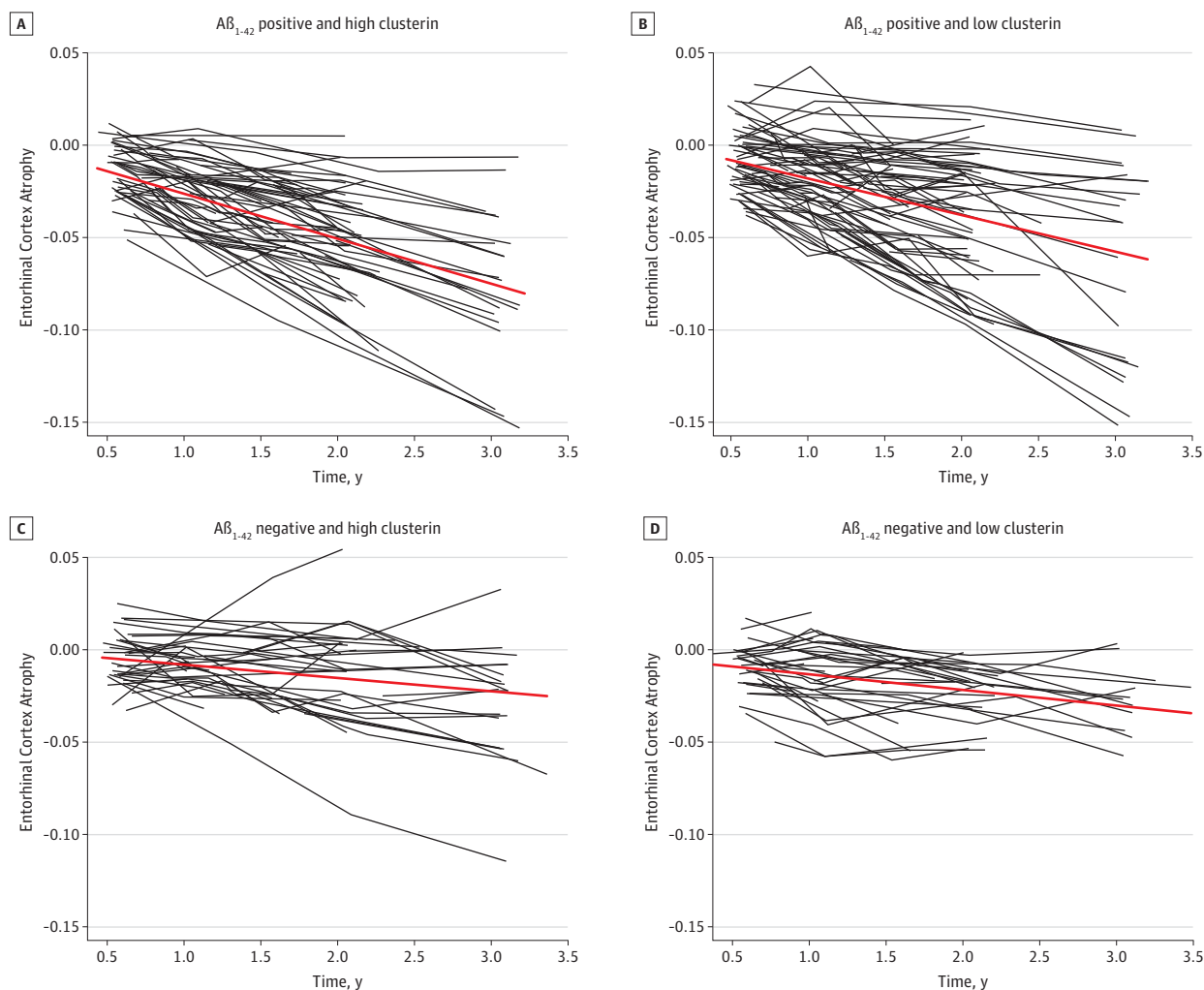
Follow-up analyses examining the 3-way interactions demonstrated that the CSF clusterin by time interaction was significantly associated with entorhinal cortex atrophy only among CSF A $\beta_{1-42}$ -positive individuals ( $\beta$  coefficient =  $-0.20$ ; SE = 0.007;  $P = .008$ ) but not among CSF A $\beta_{1-42}$ -negative individuals ( $\beta$  coefficient = 0.007; SE = 0.008;  $P = .36$ ) (Figure 3). In contrast, there was no significant CSF clusterin by time interaction on the entorhinal cortex atrophy rate either among CSF p-tau<sub>181p</sub>-positive ( $\beta$  coefficient =  $-0.01$ ; SE = 0.01;  $P = .28$ ) or among CSF p-tau<sub>181p</sub>-negative ( $\beta$  coefficient = 0.005; SE = 0.007;  $P = .49$ ) individuals (Figure 4). Similar results were obtained when CSF p-tau<sub>181p</sub> and CSF A $\beta_{1-42}$  were treated as continuous rather than categorical variables (eAppendix 2 in Supplement).

To determine whether these effects differed by group status (MCI vs HC), we performed additional analyses fitting interactions between group status and the main effects of interest (for additional details, see eAppendix 1 and eAppendix 2 in Supplement). These analyses showed a significant interaction between group status, time, CSF clusterin, and CSF A $\beta_{1-42}$  status on the entorhinal cortex atrophy rate ( $\beta$  coefficient =  $-0.031$ ; SE = 0.009;  $P = .001$ ). Follow-up subgroup analyses revealed that although both the MCI and HC cohorts demonstrated a significant 3-way interaction of time, CSF clusterin, and CSF A $\beta_{1-42}$  status on the entorhinal cortex atrophy rate, whereby entorhinal cortex volume loss was significantly associated with CSF clusterin only among CSF A $\beta_{1-42}$ -positive individuals, the slopes of change over time were steeper among the MCI cohort than the HC cohort (MCI:  $\beta$  coefficient =  $-0.076$ ; SE = 0.03;  $P = .008$ ; HC:  $\beta$  coefficient =  $-0.047$ ; SE = 0.01;  $P = .001$ ). The interaction between group status, time, CSF clusterin, and CSF p-tau<sub>181p</sub> status was not significant. Similar results were obtained when CSF p-tau<sub>181p</sub> and CSF A $\beta_{1-42}$  were treated as continuous rather than categorical variables (eAppendix 2 in Supplement).

To determine whether similar associations could be observed in other temporal lobe areas affected later in the disease process, we repeated these analyses using atrophy rates of the hippocampus, amygdala, and middle temporal gyrus.



Figure 3. Spaghetti Plots of Participants With and Without Amyloid- $\beta$  1-42 ( $A\beta_{1-42}$ )



Spaghetti plots illustrating atrophy of the entorhinal cortex among all nondemented older participants classified as  $A\beta_{1-42}$  positive and high clusterin (based on median value of clusterin) (A),  $A\beta_{1-42}$  positive and low clusterin (B),  $A\beta_{1-42}$  negative and high clusterin (C), and  $A\beta_{1-42}$  negative and low clusterin (D). The red line indicates the mean atrophy rate for the 4 respective groups (ie,  $A\beta_{1-42}$  positive and high clusterin,  $A\beta_{1-42}$  positive and low clusterin,

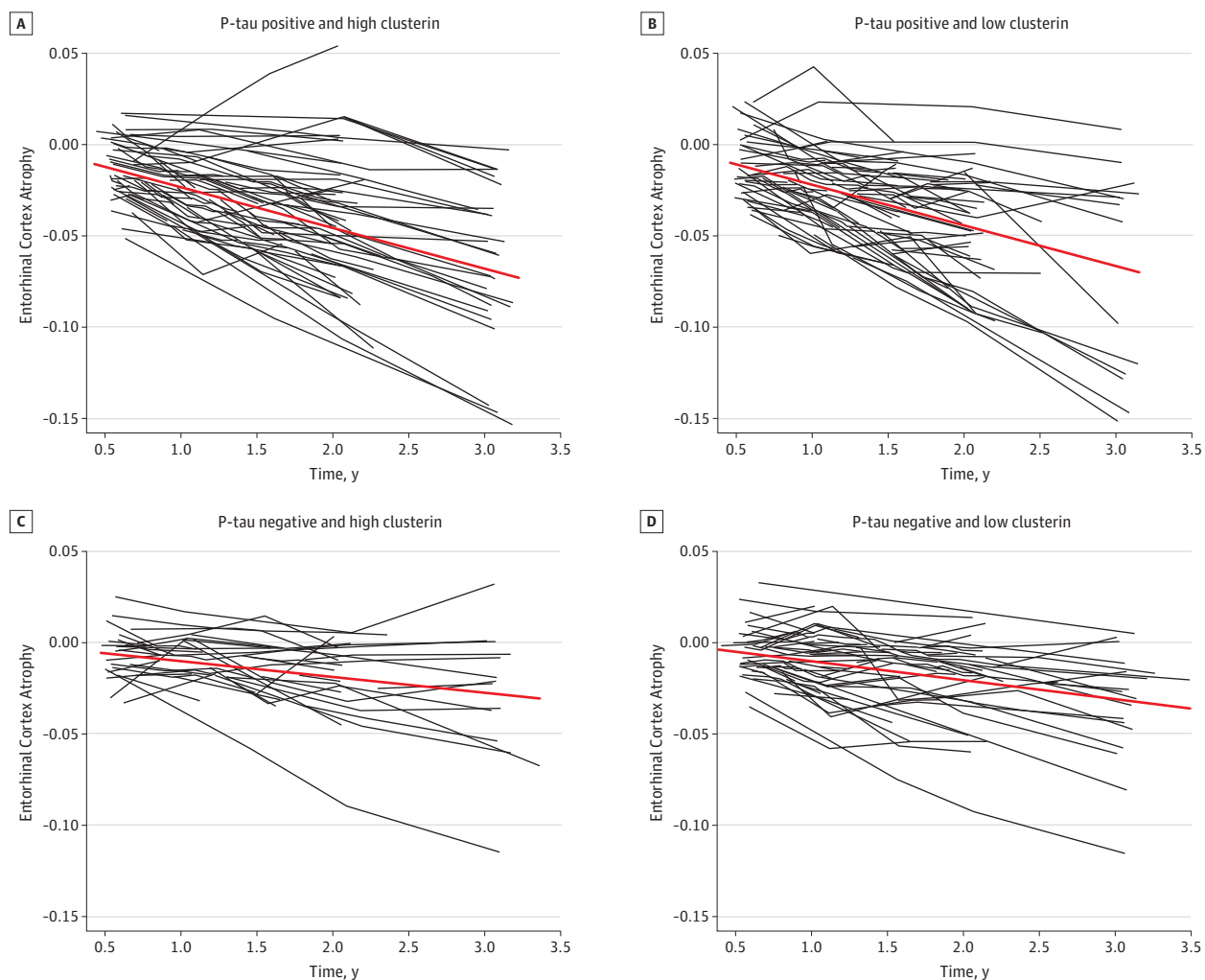
$A\beta_{1-42}$  negative and high clusterin, and  $A\beta_{1-42}$  negative and low clusterin). As illustrated in parts A and B, the slopes of the red lines between the  $A\beta_{1-42}$ -positive and high-clusterin and  $A\beta_{1-42}$ -positive and low-clusterin individuals are significantly different, corresponding to the significant interaction between cerebrospinal fluid  $A\beta_{1-42}$ , cerebrospinal fluid clusterin, and time (see text for further details).

Results revealed no significant interactions of CSF clusterin, CSF  $A\beta_{1-42}$  status, and time on the atrophy rate of the hippocampus ( $\beta$  coefficient =  $-0.013$ ; SE =  $0.01$ ;  $P = .33$ ), amygdala ( $\beta$  coefficient =  $-0.015$ ; SE =  $0.01$ ;  $P = .24$ ), and middle temporal gyrus ( $\beta$  coefficient =  $-0.009$ ; SE =  $0.01$ ;  $P = .39$ ). As observed for the entorhinal cortex atrophy rate, the interaction of CSF clusterin, CSF p-tau<sub>181p</sub> status, and time was not significant for the atrophy rate of the hippocampus ( $\beta$  coefficient =  $0.004$ ; SE =  $0.01$ ;  $P = .74$ ), amygdala ( $\beta$  coefficient =  $0.005$ ; SE =  $0.01$ ;  $P = .74$ ), and middle temporal gyrus ( $\beta$  coefficient =  $0.016$ ; SE =  $0.01$ ;  $P = .18$ ).

To determine whether the effect of clusterin on  $A\beta$ -associated neurodegeneration is independent from the previously observed effect of p-tau on  $A\beta$ -associated neurodegeneration,<sup>11-13</sup> we included interaction terms with CSF

p-tau<sub>181p</sub> status (for additional details, see eAppendix 1 and eAppendix 2 in Supplement and equation 2 in the Methods section). These analyses on the full cohort revealed significant interactions between CSF clusterin, CSF  $A\beta_{1-42}$  status, and time ( $\beta$  coefficient =  $-0.026$ ; SE =  $0.01$ ;  $P = .01$ ), as well as CSF p-tau<sub>181p</sub> status, CSF  $A\beta_{1-42}$  status, and time ( $\beta$  coefficient =  $-0.010$ ; SE =  $0.004$ ;  $P = .01$ ), on entorhinal cortex atrophy, indicating independent effects of CSF clusterin and CSF p-tau<sub>181p</sub> on CSF  $A\beta_{1-42}$ -associated volume loss. As in the primary analyses, with the interaction terms in the model, only the effect of CSF  $A\beta_{1-42}$  status by time was significant ( $\beta$  coefficient =  $0.04$ ; SE =  $0.01$ ;  $P = .009$ ); the effects of time by CSF clusterin and CSF p-tau<sub>181p</sub> status were not significant. The main effects of CSF clusterin, CSF  $A\beta_{1-42}$  status, or CSF p-tau<sub>181p</sub> status were not significant.

Figure 4. Spaghetti Plots of Participants With and Without Phosphorylated Tau (P-tau)



Spaghetti plots illustrating atrophy of the entorhinal cortex among all nondemented older participants classified as p-tau positive and high clusterin (based on median value of cerebrospinal fluid clusterin) (A), p-tau positive and low clusterin (B), p-tau negative and high clusterin (C), and p-tau negative and low clusterin (D). The red line indicates the mean atrophy rate for the 4 respective groups (ie, p-tau positive and high clusterin, p-tau positive and low

clusterin, p-tau negative and high clusterin, and p-tau negative and low clusterin). As illustrated in parts A and B, the slopes of the red lines between the p-tau-positive and high-clusterin and p-tau-positive and low-clusterin individuals are not significantly different, corresponding to the nonsignificant interaction between cerebrospinal fluid p-tau, cerebrospinal fluid clusterin, and time (see text for further details).

Additional interaction analyses with group status demonstrated significant interactions between group status, time, CSF clusterin, and CSF  $A\beta_{1-42}$  status ( $\beta$  coefficient =  $-0.020$ ; SE =  $0.003$ ;  $P = .01$ ), as well as between group status, time, CSF p-tau<sub>181p</sub> status, and CSF  $A\beta_{1-42}$  status ( $\beta$  coefficient =  $-0.008$ ; SE =  $0.003$ ;  $P = .009$ ), on the entorhinal cortex atrophy rate. Subgroup analyses showed that within the MCI cohort, interactions between both CSF clusterin, CSF  $A\beta_{1-42}$  status, and time ( $\beta$  coefficient =  $-0.047$ ; SE =  $0.02$ ;  $P = .01$ ), as well as CSF p-tau<sub>181p</sub> status, CSF  $A\beta_{1-42}$  status, and time ( $\beta$  coefficient =  $-0.014$ ; SE =  $0.007$ ;  $P = .048$ ), on entorhinal cortex atrophy were significant. Within the HC cohort, only the interaction between CSF clusterin, CSF  $A\beta_{1-42}$  status, and time on entorhinal cortex atrophy was significant ( $\beta$  coefficient =  $-0.032$ ; SE =  $0.01$ ;  $P = .02$ ); the interaction between CSF p-tau<sub>181p</sub> status, CSF  $A\beta_{1-42}$

status, and time on entorhinal cortex atrophy was not significant ( $\beta$  coefficient =  $-0.005$ ; SE =  $0.004$ ;  $P = .23$ ).

## Discussion

Here, we showed that in nondemented older individuals,  $A\beta$ -associated entorhinal cortex atrophy occurs in the presence of elevated clusterin. We also found that the effect of clusterin on  $A\beta$ -associated entorhinal cortex atrophy is not confounded or explained by p-tau. Taken together, this implicates a potentially important role for clusterin in the earliest stages of the Alzheimer neurodegenerative process and suggests independent effects of clusterin and p-tau on  $A\beta$ -associated volume loss (Figure 5).

Figure 5. Results From Linear Mixed-Effects Model

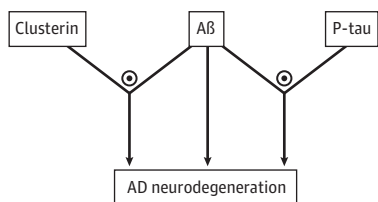


Diagram demonstrates the independent effects of clusterin and phosphorylated tau (p-tau) on Amyloid- $\beta$  (A $\beta$ )-associated volume loss in nondemented older individuals (see text for details). The circle with the dot in the center illustrates an interactive effect and the arrow demonstrates a main effect of A $\beta$ . AD indicates Alzheimer disease.

Although a number of studies have evaluated the relationship between A $\beta$ , tau, and p-tau on volume loss in the earliest stages of AD,<sup>11-15</sup> the role of clusterin in modulating this relationship is still unknown. Our findings demonstrated that nondemented older individuals with elevated CSF clusterin and decreased A $\beta$  (ie, increased intracranial A $\beta$  deposition) experience increased volume loss, suggesting that clusterin may accelerate progression from amyloid deposition to neurodegeneration. These results also indicate that a biomarker profile incorporating CSF clusterin, CSF A $\beta$ <sub>1-42</sub>, and CSF p-tau<sub>181p</sub> levels may better identify those older individuals who are at an elevated risk for progressing to dementia than any of these biomarkers by themselves.

These findings provide novel insights into the preclinical stage of AD. Although prior research suggests that clusterin by itself may not represent a marker of presymptomatic AD,<sup>6</sup> our work indicated that the presence of clusterin may represent a critical link between A $\beta$  deposition and entorhinal cortex degeneration in preclinical AD. Furthermore, in secondary analyses among HC participants, we found a significant interaction on volume loss only between clusterin and A $\beta$ , whereas among individuals with MCI, we noted concurrent interactions of A $\beta$  with both clusterin and p-tau, suggesting that the clusterin-related effects on A $\beta$ -associated neurodegeneration may precede tau-related effects. Finally, in contrast to p-tau-related atrophy within the later-affected hippocampus or other temporal lobe regions, we found clusterin-associated effects only for the entorhinal cortex, a region selectively affected in the earliest stages of AD.<sup>19</sup> Considered together, these findings indicate that the interaction between clusterin and A $\beta$  may provide an important window into the earliest stages of the Alzheimer neurodegenerative process.

Cellular and molecular evidence suggests that an interaction between clusterin and A $\beta$  potentiates neurotoxicity. Although prior experimental<sup>25</sup> and plasma-based human studies suggested that elevated clusterin levels may represent a nonetiopathologic, neuroprotective response,<sup>6,26</sup> the molecular mechanism by which clusterin affects AD pathology is still not well understood. Recent experimental evidence indicated that knockdown of clusterin protects against A $\beta$ -induced apoptosis, whereas neuronal treatment with A $\beta$  increases intracellular clusterin (and decreases extracellular clusterin), resulting in wnt/Dickkopf-1-induced neurotoxicity.<sup>27</sup> Importantly, this clusterin-dependent, wnt/Dickkopf-1-induced apoptotic effect is specific to A $\beta$  and is not observed with tau or other cytotoxic agents.<sup>27</sup> As a chaperone, clusterin has also been shown to bind with A $\beta$ , thus increasing the rate of fibrillar amyloid deposition and neuritic dystrophy<sup>28</sup> and potentiating A $\beta$  oligomeric neurotoxicity.<sup>29</sup> Consistent with these experimental results, our human findings suggest that clusterin may affect AD neurodegeneration primarily via A $\beta$ -associated mechanisms.

A limitation of our study was its observational nature, which precluded conclusions regarding causation. Our results cannot differentiate whether elevated clusterin causes, results from, or is simply correlated with amyloid deposition and entorhinal cortex atrophy. Additionally, our findings require further validation on a larger, independent population-based cohort.

## Conclusions

From a translational perspective, although considerable efforts have focused on A $\beta$  and tau, comparatively little is known about other proteins influencing Alzheimer neurodegeneration. Our findings implicate the involvement of clusterin in the earliest stages of AD. Using experimental models, it will be essential to better delineate the differential mechanistic aspects of intracellular from extracellular clusterin. In humans, it would be helpful to understand whether CSF and plasma clusterin levels correspond to experimentally derived intracellular or extracellular clusterin. It will also be important to determine whether interactions between clusterin and other factors modulate A $\beta$ -associated neurotoxicity. Along with our current findings, the results from these studies could provide valuable insights into whether modifying clusterin levels or blocking clusterin/A $\beta$  interactions are likely to represent viable therapeutic approaches for individuals in the earliest phases of the disease process.

### ARTICLE INFORMATION

**Accepted for Publication:** July 29, 2013.

**Published Online:** December 30, 2013.  
doi:10.1001/jamaneuro.2013.4560.

**Author Affiliations:** Department of Radiology, University of California, San Diego, La Jolla (Desikan, Brewer, McEvoy, Dale); Department of Psychiatry, University of California, San Diego, La Jolla (Thompson, Andreassen, Dale); Department of Neurosciences, University of California, San Diego, La Jolla (Holland, Brewer); Neuroradiology Section,

Department of Radiology and Biomedical Imaging, University of California, San Francisco (Hess); Clinical Neurochemistry Laboratory, The Sahlgrenska Academy at Göteborg University, Mölndal, Gotheburg, Sweden (Zetterberg, Blennow); University College London Institute of Neurology, Queen Square, London, England (Zetterberg); Institute of Clinical Medicine, University of Oslo and Division of Mental Health and Addiction, Oslo University Hospital, Oslo, Norway (Andreassen); Department of Neurology, Massachusetts General Hospital, Boston, Massachusetts (Hyman).

**Author Contributions:** Dr Desikan had full access to all of the data in the study and takes responsibility for the integrity of the data and the accuracy of the data analysis. Drs Desikan, McEvoy, Hyman, and Dale contributed equally. *Study concept and design:* Desikan, Andreassen, McEvoy, Hyman, Dale. *Acquisition of data:* Desikan, Holland, Zetterberg, Dale. *Analysis and interpretation of data:* All authors. *Drafting of the manuscript:* Desikan, Thompson, Holland, Andreassen, Dale.



*Critical revision of the manuscript for important intellectual content:* Desikan, Holland, Hess, Brewer, Zetterberg, Blennow, Andreassen, McEvoy, Hyman, Dale.

*Statistical analysis:* Desikan, Thompson, Dale.  
*Obtained funding:* Dale.

*Administrative, technical, or material support:* Desikan, Hess, Zetterberg, Andreassen, Dale.

*Study supervision:* Desikan, Blennow, Andreassen, McEvoy, Dale.

**Conflict of Interest Disclosures:** Dr Brewer holds stock options in CorTechs Labs Inc and serves on its advisory board, and he receives financial support from the Eli Lilly Biomarker Unit (Amyvid). Dr Brewer also receives research support from General Electric and Janssen Alzheimer Immunotherapy. Dr Blennow has served on the advisory boards for Innogenetics, Eli Lilly, Pfizer, and Roche. Dr McEvoy's spouse is the chief executive officer of CorTechs Labs Inc. Dr Dale is a founder and holds equity in CorTechs Labs Inc and serves on its scientific advisory board. The terms of this arrangement have been reviewed and approved by the University of California, San Diego, in accordance with its conflict of interest policies. No other disclosures were reported.

**Funding/Support:** This research was supported by grants from the National Institutes of Health (R01AG031224; K01AG029218; KO2 NS067427; and T32 EB005970), the Research Council of Norway (183782/V50), and the South East Norway Health Authority (2010-074). Data collection and sharing for this project was funded by the Alzheimer's Disease Neuroimaging Initiative (ADNI) (National Institutes of Health grant U01 AG024904). The ADNI is funded by the National Institute on Aging and the National Institute of Biomedical Imaging and Bioengineering, as well as through contributions from the following: Alzheimer's Association; Alzheimer's Drug Discovery Foundation; BioClinica Inc; Biogen Idec Inc; Bristol-Myers Squibb Co; Eisai Inc; Elan Pharmaceuticals Inc; Eli Lilly and Co; F. Hoffmann-La Roche Ltd and its affiliated company Genentech Inc; GE Healthcare; Innogenetics NV; IXICO Ltd; Janssen Alzheimer Immunotherapy Research & Development LLC; Johnson & Johnson Pharmaceutical Research & Development LLC; Medpace Inc; Merck & Co Inc; Meso Scale Diagnostics LLC; NeuroRx Research; Novartis Pharmaceuticals Corp; Pfizer Inc; Piramal Imaging; Servier; Synarc Inc; and Takeda Pharmaceutical Co. The Canadian Institutes of Health Research provides funds to support ADNI clinical sites in Canada. Private sector contributions are facilitated by the Foundation for the National Institutes of Health (<http://www.fnih.org>). The grantee organization is the Northern California Institute for Research and Education, and the study is coordinated by the Alzheimer's Disease Cooperative Study at the University of California, San Diego. ADNI data are disseminated by the Laboratory for Neuro Imaging at the University of California, Los Angeles. This research was also supported by National Institutes of Health grants P30 AG010129 and K01 AG030514.

**Role of the Sponsor:** The funding agencies had no role in the design and conduct of the study; collection, management, analysis, or interpretation of the data; preparation, review, or approval of the manuscript; and decision to submit the manuscript for publication.

**Additional Contributions:** Data used in preparation of this article were obtained from the Alzheimer's Disease Neuroimaging Initiative (ADNI) database (<http://adni.loni.ucla.edu>). As such, the investigators within the ADNI contributed to the design and implementation of ADNI and/or provided data but did not participate in the analysis or writing of this article.

## REFERENCES

- May PC, Johnson SA, Poirier J, Lampert-Etchells M, Finch CE. Altered gene expression in Alzheimer's disease brain tissue. *Can J Neurol Sci*. 1989;16(4)(suppl):473-476.
- McGeer PL, Kawamata T, Walker DG. Distribution of clusterin in Alzheimer brain tissue. *Brain Res*. 1992;579(2):337-341.
- Lidström AM, Bogdanovic N, Hesse C, Volkman I, Davidsson P, Blennow K. Clusterin (apolipoprotein J) protein levels are increased in hippocampus and in frontal cortex in Alzheimer's disease. *Exp Neurol*. 1998;154(2):511-521.
- Nilselid AM, Davidsson P, Nägga K, Andreassen N, Fredman P, Blennow K. Clusterin in cerebrospinal fluid: analysis of carbohydrates and quantification of native and glycosylated forms. *Neurochem Int*. 2006;48(8):718-728.
- Yu JT, Tan L. The role of clusterin in Alzheimer's disease. *Mol Neurobiol*. 2012;45(2):314-326.
- Schrijvers EM, Koudstaal PJ, Hofman A, Breteler MM. Plasma clusterin and the risk of Alzheimer disease. *JAMA*. 2011;305(13):1322-1326.
- Thambisetty M, Simmons A, Velayudhan L, et al. Association of plasma clusterin concentration with severity, pathology, and progression in Alzheimer disease. *Arch Gen Psychiatry*. 2010;67(7):739-748.
- Freeman SH, Kandel R, Cruz L, et al. Preservation of neuronal number despite age-related cortical brain atrophy in elderly subjects without Alzheimer disease. *J Neuropathol Exp Neurol*. 2008;67(12):1205-1212.
- Bobinski M, de Leon MJ, Wegiel J, et al. The histological validation of post mortem magnetic resonance imaging-determined hippocampal volume in Alzheimer's disease. *Neuroscience*. 2000;95(3):721-725.
- Blennow K, Zetterberg H, Fagan AM. Fluid biomarkers in Alzheimer disease. *Cold Spring Harb Perspect Med*. 2012;2(9):a006221.
- Desikan RS, McEvoy LK, Thompson WK, et al; Alzheimer's Disease Neuroimaging Initiative. Amyloid- $\beta$  associated volume loss occurs only in the presence of phospho-tau. *Ann Neurol*. 2011;70(4):657-661.
- Desikan RS, McEvoy LK, Thompson WK, et al; Alzheimer's Disease Neuroimaging Initiative. Amyloid- $\beta$ -associated clinical decline occurs only in the presence of elevated p-tau. *Arch Neurol*. 2012;69(6):709-713.
- Desikan RS, McEvoy LK, Holland D, et al; Alzheimer's Disease Neuroimaging Initiative. Apolipoprotein E epsilon4 does not modulate amyloid- $\beta$ -associated neurodegeneration in preclinical Alzheimer disease. *AJNR Am J Neuroradiol*. 2013;34(3):505-510.
- Storandt M, Head D, Fagan AM, Holtzman DM, Morris JC. Toward a multifactorial model of Alzheimer disease. *Neurobiol Aging*. 2012;33(10):2262-2271.
- Stricker NH, Dodge HH, Dowling NM, Han SD, Erosheva EA, Jagust WJ; Alzheimer's Disease Neuroimaging Initiative. CSF biomarker associations with change in hippocampal volume and precuneus thickness. *Brain Imaging Behav*. 2012;6(4):599-609.
- Alzheimer's Disease Neuroimaging Initiative. *Biomarkers Consortium Data Primer Version December 28, 2011*. La Jolla, CA: Alzheimer's Disease Neuroimaging Initiative.
- Shaw LM, Vanderstichele H, Knopik-Czajka M, et al; Alzheimer's Disease Neuroimaging Initiative. Cerebrospinal fluid biomarker signature in Alzheimer's Disease Neuroimaging Initiative subjects. *Ann Neurol*. 2009;65(4):403-413.
- Fennema-Notestine C, Hagler DJ Jr, McEvoy LK, et al; Alzheimer's Disease Neuroimaging Initiative. Structural MRI biomarkers for preclinical and mild Alzheimer's disease. *Hum Brain Mapp*. 2009;30(10):3238-3253.
- Braak H, Braak E. Neuropathological staging of Alzheimer-related changes. *Acta Neuropathol*. 1991;82(4):239-259.
- Desikan RS, Ségonne F, Fischl B, et al. An automated labeling system for subdividing the human cerebral cortex on MRI scans into gyral based regions of interest. *Neuroimage*. 2006;31(3):968-980.
- Fischl B, Salat DH, Busa E, et al. Whole brain segmentation: automated labeling of neuroanatomical structures in the human brain. *Neuron*. 2002;33(3):341-355.
- Holland D, Dale AM; Alzheimer's Disease Neuroimaging Initiative. Nonlinear registration of longitudinal images and measurement of change in regions of interest. *Med Image Anal*. 2011;15(4):489-497.
- Holland D, McEvoy LK, Dale AM; Alzheimer's Disease Neuroimaging Initiative. Unbiased comparison of sample size estimates from longitudinal structural measures in ADNI. *Hum Brain Mapp*. 2012;33(11):2586-2602.
- Morris JC. The Clinical Dementia Rating (CDR): current version and scoring rules. *Neurology*. 1993;43(11):2412-2414.
- Nuutinen T, Suuronen T, Kauppinen A, Salminen A. Clusterin: a forgotten player in Alzheimer's disease. *Brain Res Rev*. 2009;61(2):89-104.
- Thambisetty M, An Y, Kinsey A, et al. Plasma clusterin concentration is associated with longitudinal brain atrophy in mild cognitive impairment. *Neuroimage*. 2012;59(1):212-217.
- Killick R, Ribe EM, Al-Shawi R, et al. Clusterin regulates  $\beta$ -amyloid toxicity via Dickkopf-1-driven induction of the wnt-PCP-JNK pathway [published online November 20, 2012]. *Mol Psychiatry*. doi:10.1038/mp.2012.163.
- DeMattos RB, O'dell MA, Parsadanian M, et al. Clusterin promotes amyloid plaque formation and is critical for neurotoxicity in a mouse model of Alzheimer's disease. *Proc Natl Acad Sci U S A*. 2002;99(16):10843-10848.
- Lambert MP, Barlow AK, Chromy BA, et al. Diffusible, nonfibrillar ligands derived from Abeta1-42 are potent central nervous system neurotoxins. *Proc Natl Acad Sci U S A*. 1998;95(11):6448-6453.